Quantized Auger recombination of biexcitons in CdSe nanorods studied by time-resolved photoluminescence and transient-absorption spectroscopy

Seiji Taguchi,[1] Masaki Saruyama,[2] Toshiharu Teranishi,[2] and Yoshihiko Kanemitsu[1,3,*]

[1]*Institute for Chemical Research, Kyoto University, Uji, Kyoto 611-0011, Japan*
[2]*Department of Chemistry, Graduate School of Pure and Applied Sciences, University of Tsukuba, Tsukuba, Ibaraki 305-8571, Japan*
[3]*Photonics and Electronics Science and Engineering Center, Kyoto University, Kyoto 615-8510, Japan*

We studied the recombination dynamics of biexcitons in elongated CdSe nanocrystals (nanorods) using time-resolved photoluminescence (PL) and transient absorption (TA) spectroscopy. The decay times of the PL and TA signals decrease with increasing nanorod length. Under weak excitation, the PL decay is faster than the TA decay, and the nonradiative hole trapping determines the PL decay in several hundreds of picoseconds. Under intense excitation, the PL decay curves are similar to the TA decay curves, and the rapid biexciton decay is caused by nonradiative Auger recombination. A clear correlation is observed between the Auger recombination coefficient of the biexcitons and the average PL lifetime of the single excitons. Moreover, the Auger recombination lifetimes of the biexcitons are shorter in nanorods than in spherical nanocrystals of the same volume. Our study clarified that the Auger recombination rate is strongly affected by a high surface-state density.

I. INTRODUCTION

Over the past two decades, semiconductor nanocrystals (NCs) have been studied intensively because they show size-dependent and fascinating optical and electronic properties.[1–4] The optical properties of NCs can be tailored by controlling their size, shape, and composition. Additionally, semiconductor NCs provide a stage for experimental studies of many-body effects on optical processes for electrons and excitons in nanoscale materials. Strongly confined electrons and excitons in NCs show unique nonlinear optical properties compared with semiconductor bulk crystals.[5] Charge-carrier confinement and reduced dielectric constants in small NCs enhance the carrier-carrier Coulomb interactions, leading to efficient multiparticle processes. Recent time-resolved femtosecond spectroscopy studies have shown unique carrier relaxation processes, such as quantized Auger recombination[6–15] (the electron–hole recombination energy is transferred to another electron or hole) and multiple-exciton generation (a single photon creates two or more electron-hole pairs).[16–20] In particular, the Auger process causes very rapid nonradiative recombination of multiple electron-hole (e-h) pair states in NCs, leading to luminescence degradation[21] and luminescence blinking.[22–24] Understanding the mechanism of Auger recombination is significant in fundamental physics and NC applications.

The Auger decay rate in semiconductor NCs depends strongly on the NC size. In spherical NCs, it has been reported that the Auger lifetime is proportional to the NC volume.[6] This volume effect has been confirmed for a variety of NCs, including CdSe, PbSe, Ge, and InAs.[7,8,12,14] In small spherical NCs with radii of a few nanometers, the Auger recombination can be treated as a three-particle collision (electron-hole-electron or electron-hole-hole) rather than a two-particle collision (exciton-exciton).[6,11] The Auger lifetime is inversely proportional to the square of the effective carrier density and is proportional to the square of the NC volume. The empirical linear scaling with NC volume is explained by the finite density of states in the NCs where residual carriers are transferred. On the other hand, because NCs have large surface-to-volume ratios, their optical properties are sensitive to the surface structure and the surrounding environment.[25–27] For example, photoluminescence (PL) blinking behavior can be drastically varied by controlling the surface structure and the local environment,[22,23,28–30] where the Auger recombination plays a dominant role in PL blinking. Recently, the nonradiative Auger recombination rate was significantly reduced by the formation of smooth potential boundaries in NCs with a core/shell alloy interface, leading to suppression of PL blinking and luminescence from higher exciton states.[31–33] Moreover, a recent study showed that the Auger lifetime and its size dependence were influenced by surface capping ligands in CdTe NCs.[13] These observations indicate that surface states are important in nonradiative Auger recombination processes in NCs.

Here, we anticipate that elongated NCs [nanorods (NRs)] are a model material for clarifying the surface-state effects on the Auger recombination rate. Elongated structures such as NRs have a high fraction of surface atoms, whereas spherical NCs have the lowest fraction of surface atoms. Thus, surface effects on optical processes should be enhanced in NRs. In fact, the Auger lifetimes are shorter in NRs than in spherical NCs of the same volume.[34] However, in one-dimensional quantum wire structures, such as long NRs with large aspect ratios, the mechanism of Auger recombination becomes a two-particle exciton-exciton collision.[34,35] We used short NRs with small aspect ratios (elongated NCs with short lengths) to reduce the zero- to one-dimensional transformation effects on multiparticle Auger recombination; thus, the Auger recombination can be treated as a three-particle process.

In this work, we studied the recombination dynamics of biexcitons (two e-h-pair states) in CdSe NRs. The biexciton lifetimes in short NRs were measured using time-resolved PL spectroscopy and transient absorption (TA) spectroscopy. Under weak excitation, PL decay times decrease with increasing aspect ratio, and they are determined by single-carrier trapping at the NR surface. Under intense excitation, the

biexciton lifetimes are determined by nonradiative Auger recombination. The biexciton lifetimes are shorter in NRs than in spherical NCs of the same volume. We found that the effective Auger coefficient in NRs is approximately proportional to the hole-trapping rate, indicating that the surface states influence the three-particle Auger recombination process in short NRs with small aspect ratios.

II. EXPERIMENT

Alkyl-phosphonic-acid-capped CdSe NRs were synthesized using a previously reported organometallic approach with minor modifications.[36] Typically, 4.1-nm-wide and 10.1-nm-long CdSe NRs were synthesized as follows. CdO (64 mg, 0.5 mmol), octadecylphosphonic acid (334 mg, 1.0 mmol), and tri-n-octylphosphine oxide (1 g) were loaded into the reaction flask and heated to 350 °C under nitrogen atmosphere until the CdO reacted to give a transparent solution. A tri-n-octylphosphine (1 ml) solution of Se (30 mg, 0.38 mmol) was swiftly injected into the reaction flask at 320 °C, and the resulting CdSe NRs were allowed to grow for 20 min at 250 °C. The CdSe NRs were purified by precipitation and centrifugation with an excess of ethanol and redispersed in hexane. The CdSe NR length was precisely controlled by varying the injection rate, reaction temperature, and growth time. The NR diameters (D) were ~4 nm, and the length along the rod axis (L) was varied. We used four different NR samples: $D \times L = 4.1$ nm $\times 10.1$ nm, 3.9 nm $\times 14.3$ nm, 3.9 nm $\times 19.4$ nm, 4.0 nm $\times 23.5$ nm. Typical transmission electron microscopy (TEM) images are shown in Figs. 1(a) and 1(b). For comparison, spherical CdSe NCs with $D = 2.0$ nm, 3.0 nm (Ref. 37), 4.2 nm (Ref. 38), 5.0 nm (Ref. 39), and 6.1 nm (Ref. 40) were also synthesized as described previously, with minor modifications: CdSe NCs with $D = 2.0$ and 3.0 nm were capped with myristic acid, those with $D = 4.2$ nm were capped with a mixture of octanoic acid, oleylamine, and tri-n-octylphosphine, those with $D = 5.0$ nm were capped with a mixture of oleic acid, oleylamine, and tri-n-octylphosphine, and those with $D = 6.1$ nm were capped
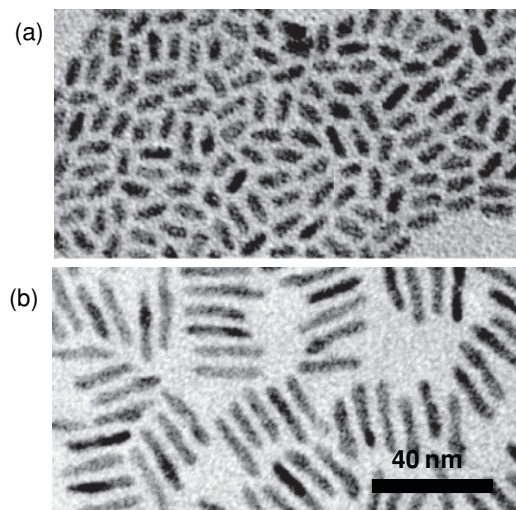
with oleic acid. The size dispersions for diameter and length of our NR samples were ~10%, and those for diameter of our spherical NC samples were <15%. All samples were dispersed in n-hexane after iterated washing using acetone and ethanol.

We studied ultrafast carrier dynamics in CdSe NCs and NRs using time-resolved PL and pump-probe TA spectroscopy. The light source was a regenerative amplified mode-locked Ti:sapphire laser with a pulse duration of 150 fs and a repetition rate of 1 kHz. We used 400 nm (3.1 eV) pulses for the pump light. Time-resolved PL spectra were measured using a streak camera with a monochromator. The typical time resolution in PL measurements was about 50 ps. For TA measurements, we used probe pulses with photon energies tuned to the lowest excitonic absorption resonance and monitored the state-filling-induced absorption bleaching as a function of the average number of photocreated e-h pairs per NR. In all measurements, we used n-hexane solutions of NRs and NCs in a 1-mm-thick quartz cell. The sample solutions were vigorously stirred using a magnetic stirrer to reduce photodegradation and charging. All measurements were carried out at room temperature.

III. RESULTS AND DISCUSSION

A. Hole trapping at the surface

Figure 2 shows linear optical absorption and time-integrated PL spectra of the spherical NC sample ($D = 4.2$ nm) and the NR samples with different lengths L. In all samples used in this work, a clear absorption peak and a PL band were observed due to the lowest exciton. The NR diameters are almost the same, but small changes of peak energies of the lowest exciton in NRs are caused by the small variation in the NR diameter

FIG. 1. Transmission electron microscope images of CdSe NRs with a rod length of $L =$ (a) 10.1 and (b) 23.5 nm.
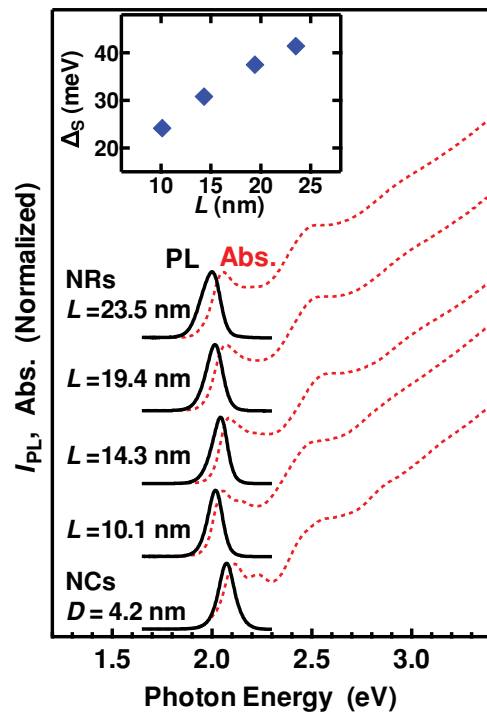

FIG. 2. (Color online) Linear optical absorption (broken red curves) and PL spectra (solid black curves) of spherical NCs and elongated NRs. Inset: Stokes shift Δ_S as a function of L.

in our samples. The peak energies are determined by the NR diameter rather than NR length. The confinement energy is predominantly determined by the dimension perpendicular to the rod axis because the rod length was larger than the exciton Bohr radius of the CdSe crystals in the NRs. Thus, the confinement energies are almost independent of the rod length.

The inset in Fig. 2 shows the Stokes shift of NRs, Δ_S, as a function of L. The Stokes shift between the PL and absorption peaks increases with L and is smaller than about 40 meV. This is consistent with the previous report of CdSe NRs.[41] Therefore, the observed absorption and PL bands originate from the lowest exciton states rather than from the shallow-trap states.

Figure 3(a) shows the temporal evolution of the PL intensity in the NRs at weak excitation intensities. The average number of photocreated e-h pairs per NR, $\langle N_0 \rangle$, was calculated from the absorption cross section, and its value was less than 0.1. Thus, multiparticle (or multiexciton) effects on the PL dynamics were negligible under these conditions. Here, the absorption cross sections of our NR samples were determined using rapid Auger recombination, as shown in Sec. III B. The rapid PL decay for the NRs occurs in ~1 ns, whereas the radiative lifetime of the spherical CdSe NCs is ~20 ns.[42] The PL decay becomes faster with increasing rod length, as shown in Fig. 3(a). Because the PL decay curves are not exponential, we fitted the PL decay curves using triple-exponential functions, $A_1 \exp(-t/\tau_1) + A_2 \exp(-t/\tau_2) + A_3 \exp(-t/\tau_3)$, convoluted

by the Gaussian instrument response function, and we defined the average PL lifetime of single excitons, $\langle \tau_{PL} \rangle$, as $(A_1 \tau_1 + A_2 \tau_2 + A_3 \tau_3)/(A_1 + A_2 + A_3)$. As shown by the solid curves in Fig. 3(a), the observed curves can be fitted well by triple-exponential functions. In our samples, τ_1 is a few tens of picoseconds, τ_2 is a few hundreds of picoseconds, and τ_3 is a few nanoseconds. Because the origin of these three lifetimes is not clear, hereafter we discuss the PL decay dynamics using the average PL lifetime $\langle \tau_{PL} \rangle$. In longer NRs with larger surface area, the average exciton PL decay rate $\langle \tau_{PL} \rangle^{-1}$ is larger, indicating that the NR surface affects the rapid PL decay [Fig. 3(b)].

A large discrepancy was observed between PL and TA decay curves at weak excitation intensities. Figure 3(c) shows the PL and TA decay curves for the NR sample with $L=$ 10.1 nm under weak excitation, where both PL and TA intensities were normalized at zero time delay. The PL decay is faster than the TA decay due to the difference between the carrier decay processes monitored using the two methods. The PL intensity I_{PL} is proportional to the number of e-h pairs (bimolecular radiative recombination). In contrast, the TA intensity variation due to state-filling-induced bleaching is proportional to the sum of the occupation numbers of quantized electron and hole states. Due to the large degeneracy of the valence band and the large difference between electron and hole masses [$m_e = 0.13m_0$, $m_h = 2.5m_0$ ($//c$) and $0.45m_0$ ($\perp c$)] in CdSe,[43] the hole population is spread over many levels near the lowest states by thermal distribution.[44] At room temperature, the occupation probability of the lowest electron state is much greater than that of the lowest hole state. As a result, the TA dynamics is predominantly determined by the electron decay dynamics.[44] When the hole depopulates at the lowest states, absorption bleaching occurs due to the electron state filling, but the PL disappears. We fitted the PL and TA decay curves in Fig. 3(c) using triple-exponential functions, and obtained the weighted average lifetimes of 1.7 and 3.2 ns for PL and TA decay curves, respectively. The difference between the TA and PL decays in Fig. 3(c) indicates that the rapid PL decay at the initial stage is determined by the hole depopulation of the lowest state. Under weak excitation, the hole depopulation of the lowest state is faster than the electron depopulation of the lowest state. Thus, the nonradiative hole trapping determines the PL decay at the initial stage.

Klimov *et al.* reported that the origin of ultrafast hole trapping in a few picoseconds is not defect related, but is intrinsic to the NC because the hole depopulation dynamics is independent of the NC surface properties.[44] Similar ultrafast PL decay components in a few picoseconds have also been reported as independent of the ZnS overcoating.[45] However, the PL lifetimes observed in our NRs show a clear dependence on surface area. Moreover, Jiang and Kelley reported that the PL lifetime depend on surface-capping ligands to CdSe NRs synthesized by a very similar method.[46] Thus, our average PL lifetimes are determined by hole trapping at surface-localized states rather than by the rapid and intrinsic hole trapping in the NC interior. If the rapid PL decay results from the hole trapping at surface states, the PL decay-curve profile depends on the surface-state density. The NR samples are inhomogeneous because each NR has a different number of surface states and a variation of hole-trapping rates. Thus, nonexponential
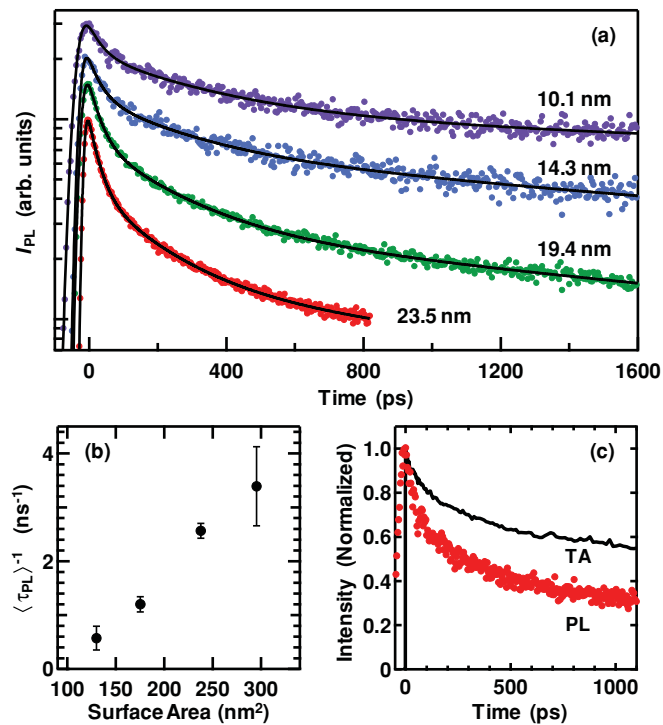

FIG. 3. (Color online) (a) The temporal evolution of PL intensities of CdSe NRs with different rod lengths. Black curves show triple-exponential fitting results. (b) Average PL decay rate as a function of the NR surface area. (c) Carrier relaxation dynamics in $L=10.1$ nm NRs measured by PL (red circles) and TA (solid black curve).

PL decay was observed in ensemble-averaged experiments. Jones *et al*. also explained the wide-ranging multiexponential PL decay by considering the carrier transfer into surface defect sites based on Marcus theory.[47] From the above considerations, we concluded that the nonexponential PL decay with lifetime from 300 ps to 1.7 ns indicates single-hole trapping at surface states under weak excitation.

B. Biexciton decay and the Auger recombination coefficient

Figure 4(a) shows the PL decay curves in CdSe NRs for $L = 10.1$ nm (upper traces) and 19.4 nm (lower traces) at various excitation intensities. All curves were normalized by the PL intensities at the delay time of 1.3 ns. With increasing $\langle N_0 \rangle$, the rapid-decay component appears within several hundreds of picoseconds. The long-decay component $\geqslant 1$ ns does not depend on the excitation intensity. Figure 4(b) shows the PL spectra for NRs of $L = 10.1$ nm just after the excitation ($t = 0$ ns) and at a long delay ($t = 1.5$ ns), during which the rapid-decay component diminishes [see Fig. 4(a)]. All spectra were normalized by the peak values. Under high excitation intensity ($\langle N_0 \rangle = 1.0$, upper traces), a redshift of the PL spectrum at $t = 0$ ns was observed, whereas the PL spectrum at $t = 1.5$ ns was not redshifted. However, no redshift was observed under low excitation intensity ($\langle N_0 \rangle = 0.07$, lower traces). Thus, this redshift at the initial decay stage results from the biexciton binding energy, indicating that the rapid decay just after the photoexcitation originates from biexciton recombination.[48]
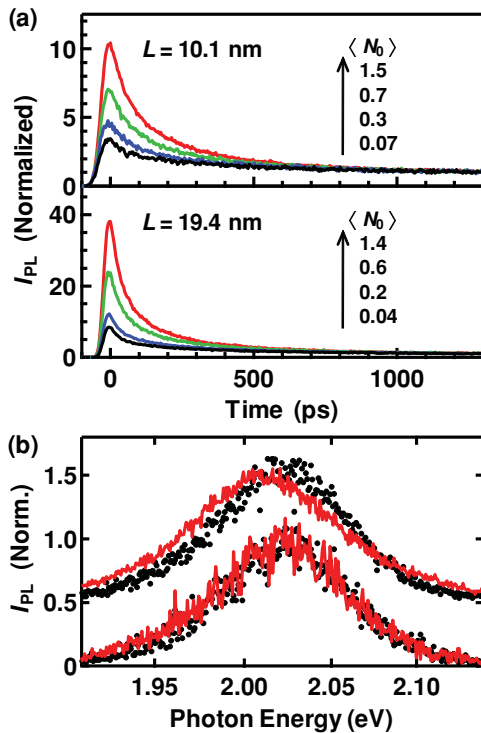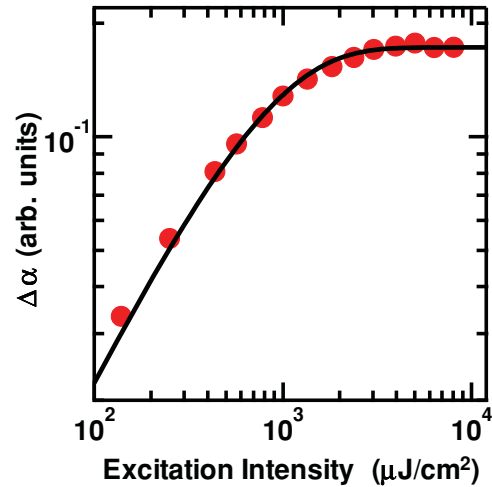

FIG. 5. (Color online) TA signal intensities at the delay time of 1.2 ns as a function of the excitation intensity for $L = 10.1$ nm NRs. Black curve shows the fitting results, assuming the Poisson distribution of the number of initially photocreated *e-h* pairs.

To gain a deeper understanding of the biexciton decay dynamics, we examined the TA decay dynamics of NRs and compared the PL data with the TA data. Figure 5 shows the TA intensity at the delay time of 1.2 ns as a function of the excitation intensity for $L = 10.1$ nm NRs. Since a rapid recombination occurs within a few hundreds of picoseconds in highly excited NRs, we consider that almost all excited NRs contain only a single *e-h* pair at a long delay time of 1.2 ns. Assuming that the probability of the number of initially created *e-h* pairs is described by the Poisson distribution, the TA intensity is proportional to $1 - e^{-\langle N_0 \rangle}$.[12,15] By fitting the TA signals at 1.2 ns, we evaluated the absorption cross section of 7.0×10^{-16} cm^2 in the $L = 10.1$ nm NRs.

Figure 6(a) compares the carrier dynamics measured by TA in spherical NCs ($D = 6.1$ nm) with those in NRs ($L = 10.1$ nm). The dimensions of the NCs and NRs were designed to have nearly the same volume, and the decay curves were normalized by the TA intensity at the delay time of 1.3 ns. In both samples, the rapid-decay component due to the biexcitons appears with increasing excitation intensities. The biexciton decay in the NRs is faster than that in the NCs, although the carrier densities of both samples are the same.

By subtracting the decay profiles at lower densities from those at higher densities, the biexciton recombination components can be discussed.[6] Figure 6(b) shows the extracted TA signals of the NRs and NCs. The biexciton lifetimes ($\sim$410 ps in spherical NCs and $\sim$160 ps in NRs) were evaluated using single-exponential fitting. All curves extracted from the decay profiles under various excitation conditions [red circles and black broken line in Fig. 6(b) for $L = 10.1$ nm NRs] are very similar within experimental error, indicating that the biexciton lifetimes in the NRs and NCs are quantized.

Figure 7 shows the biexciton decay curves in the NRs ($L = 14.3$ and 19.4 nm) evaluated from PL (black solid circles) and TA (blue open circles) measurements using a subtraction procedure. Under intense excitation, the biexciton decay curves extracted from PL measurements are very similar to those from TA measurements in the $L = 10.1$, 14.3, and

FIG. 4. (Color online) (a) The excitation intensity dependence of PL decay dynamics in $L = 10.1$ (upper traces) and 19.4 nm (lower traces) NRs. (b) PL spectra at $t = 0$ (red curves) and 1.5 ns (black circles). The excitation intensity was $\langle N_0 \rangle = 1.0$ (upper traces) and 0.07 (lower traces).
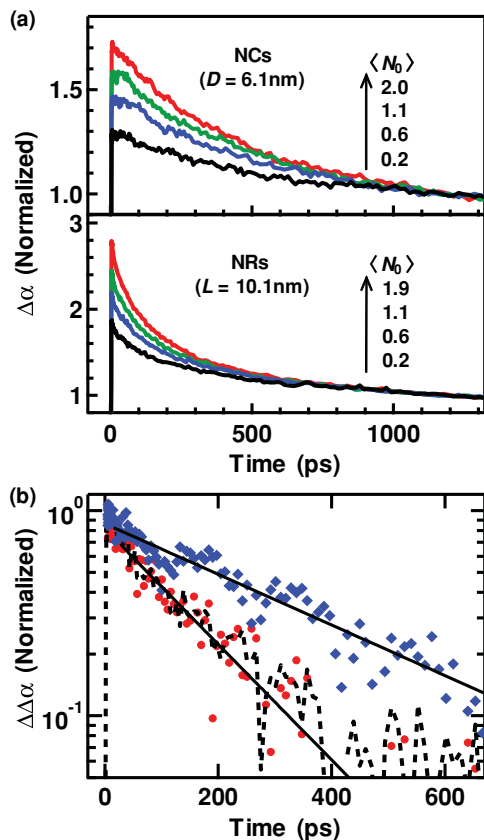
FIG. 6. (Color online) (a) The temporal evolution of TA signal intensities of $D = 6.1$ nm spherical NCs (upper traces) and $L = 10.1$ nm NRs (lower traces) at several excitation intensities. The volumes of the NCs and NRs are almost the same. (b) The biexciton decay components of the $D = 6.1$ nm spherical NCs (blue diamonds) and the $L = 10.1$ nm NRs (red circles) extracted from TA results using the subtraction procedure. Broken black curve shows that of $L = 10.1$ nm NRs extracted by another set of TA decay profiles at different excitation intensities. Solid black lines show fitting results.

19.4 nm NR samples. Note that a large discrepancy between the PL and TA decays was observed under weak excitation conditions, as discussed in Sec. III A. The similarity in the decay curves for TA and PL signals indicates that electrons and holes simultaneously depopulate in the lowest states, and the biexciton decay dynamics is determined by intrinsic *e-h* pair recombination. In addition, the radiative lifetimes of biexcitons can be estimated at 5–10 ns from the ∼20 ns radiative lifetime of single excitons in CdSe NCs.[42] Based on the subnanosecond biexciton lifetime, we concluded that the rapid recombination of biexcitons is caused by nonradiative Auger recombination.

The biexciton decay curves observed in longer NRs are nonexponential. We can approximately fit the decay curves using a double-exponential function, $f(t) = A_\mathrm{f}\exp(-t/\tau_\mathrm{f}) + A_\mathrm{s}\exp(-t/\tau_\mathrm{s})$. The average biexciton lifetime $\langle\tau_\mathrm{BX}\rangle$ is defined as $(A_\mathrm{f}\tau_\mathrm{f} + A_\mathrm{s}\tau_\mathrm{s})/(A_\mathrm{f} + A_\mathrm{s})$. Figure 8(a) summarizes the biexciton lifetimes of the spherical NCs measured by TA and the NRs by TA and PL as functions of their volumes. In spherical NCs, the biexciton lifetime increases with increasing NC volume. In smaller NCs, the biexciton lifetime approximately scales linearly with the NC volume, as previously reported.[6] The broken line shows a guide for spherical NCs.
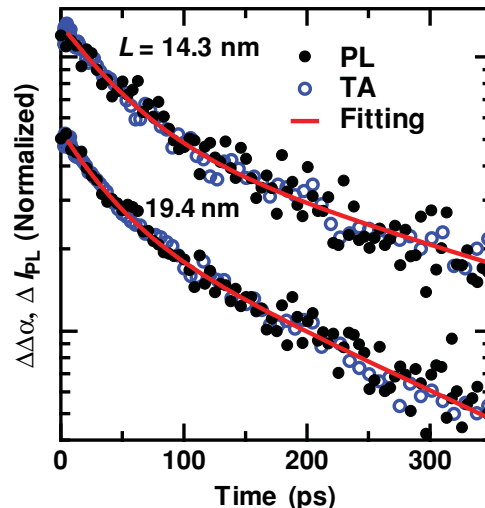

FIG. 7. (Color online) Biexciton relaxation components extracted from PL (black circles) and TA (blue open circles) results by the subtraction procedure. Red curves show fitting results using the double-exponential function.

In contrast, the NR biexciton lifetime depends weakly on or is almost independent of the NR volume. Moreover, the average biexciton lifetimes in the NRs are shorter than in the spherical NCs of the same volume (see Fig. 6), indicating that the NRs have larger Auger recombination rates. A similar difference in the biexciton lifetimes between NCs and NRs has been reported by Htoon *et al.*[34] In their TA experiments, they used longer NRs with large aspect ratios and concluded that one-dimensional exciton-exciton collision occurs in long NRs. Therefore, we need to consider two elongated-shape effects on the multicarrier recombination dynamics in short NRs: (i) the transformation effect from zero- to one-dimensional structures and (ii) the surface effect. According to Ref. 34, in our short NRs where the aspect ratio is less than about 6, the Auger recombination can be treated as a three-particle collision (electron-hole-electron or electron-hole-hole) rather than a two-particle collision (exciton-exciton). Here we consider that the large NR surface area rather than one-dimensional excitonic behavior alters the Auger recombination rate in short NRs.

To quantitatively examine the Auger recombination rate, we estimated an effective Auger recombination coefficient C_A, which is defined as $C_\mathrm{A} = \tau_\mathrm{BX}^{-1}(2/V)^{-2}$, where τ_BX and V are the biexciton lifetime and volume, respectively.[6] We assumed that the Auger recombination involves a three-particle collision process and photocreated *e-h* pairs are treated as independent particles rather than as correlated excitons. Figure 8(b) shows the calculated C_A as a function of the average PL decay rate $\langle\tau_\mathrm{PL}\rangle^{-1}$, which depended on the NR surface area, reflecting the hole-trapping rate, as discussed in the previous section. The values of C_A in our NRs are remarkably larger than the Auger coefficient of a bulk CdSe crystal (∼1.1×10^{-30} s^{-1} cm^6)[49] as well as those of the spherical NCs. Thus, the Auger recombination coefficient is enhanced due to the large surface area of the NRs. We found a good linear correlation between C_A and $\langle\tau_\mathrm{PL}\rangle^{-1}$, indicating that the Auger recombination in short NRs is strongly affected by the number of
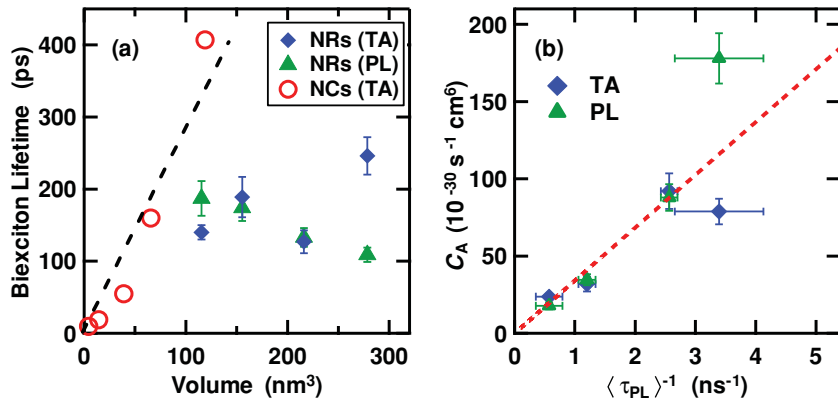
FIG. 8. (Color online) (a) Biexciton life-times in NRs measured by time-resolved PL (green triangles) and TA (blue diamonds) and in spherical NCs by TA (red circles). The broken line shows the guide for the spherical NCs. (b) Auger coefficient of NRs as a function of the average PL decay rate $(\langle \tau_{PL} \rangle^{-1})$.

surface-localized states. In long NRs, a one-dimensional exciton nature would become essential.[34] Thus, we conclude that both large surface area and one-dimensional exciton-exciton collisions play an important role in determining the Auger recombination rate in NRs.

We found that the surface-localized states influence the Auger recombination process in short NRs; Auger recombination rates increase with increasing number of surface-localized states. Here, we consider two potential roles of the surface-localized states: (i) a trap-assisted Auger process (Ref. [50]) and (ii) an increase in the final state number in the Auger process. In donor-doped semiconductors, for example, a three-particle collision occurs between a donor electron, a free electron, and a free hole.[50] In this trap-assisted Auger process for NRs, the rapid carrier trapping at surface states should occur prior to the three-particle collision of Auger processes. In this case, the biexciton recombination dynamics should be determined by the surface hole trapping rather than by following *e-h* recombination. However, the same biexciton decay curves were extracted from PL and TA measurements, and the biexciton decay is faster than the surface trapping of holes, indicating that the biexciton decays are determined by the recombination of delocalized *e-h* pairs rather than hole trapping at localized states. Thus, it is unlikely that the trap-assisted Auger process occurs in our experiments. At present, we believe that the surface states cause the increase in the final state number of the Auger recombination process. Residual carriers transform the energy released in the recombination of delocalized electrons and holes into kinetic energy, which are scattered into surface-localized states. This is considered as "Auger-assisted carrier trapping." In NRs, the Auger recombination rate is enhanced by the large number

of final states due to the large surface area. This model can explain the nonexponential biexciton decay, which results from inhomogeneous variations in the surface-state numbers of individual NRs. Thus, the Auger recombination rate is affected by the surface state of the NRs.

IV. CONCLUSION

We studied biexciton recombination mechanisms in CdSe NRs, where quantum confinement is treated as zero dimensional. A comparison of the dynamics measured by PL and TA shows that the single-exciton lifetime is determined by hole trapping, and the biexciton lifetime is determined by quantized Auger recombination. The hole-trapping rate increases with increasing rod length, indicating that holes are trapped by surface states. The biexciton lifetime depends on the size and shape of the NCs. The effective Auger coefficient of the NRs is proportional to the hole-trapping rate at surface states. We concluded that in short NRs with small aspect ratios the biexciton decay is enhanced by the surface trapping of Auger carriers. Auger recombination in NRs with large surface area is a multicarrier recombination process involving quantized interior states inside the NCs as well as surface-localized states.

*Corresponding author: kanemitu@scl.kyoto-u.ac.jp

[1] L. Brus, J. Phys. Chem. **90**, 2555 (1986).

[2] Y. Kanemitsu, Phys. Rep. **263**, 1 (1995).

[3] A. P. Alivisatos, J. Phys. Chem. **100**, 13226 (1996).

[4] S. A. Empedocles, R. Neuhauser, K. Shimizu, and M. G. Bawendi, Adv. Mater. **11**, 1243 (1999).

[5] V. I. Klimov, J. Phys. Chem. B **110**, 16827 (2006).

[6] V. I. Klimov, A. A. Mikhailovsky, D. W. McBranch, C. A. Leatherdale, and M. G. Bawendi, Science **287**, 1011 (2000).

[7] B. Fisher, J. Caruge, Y. Chan, J. Halpert, and M. G. Bawendi, Chem. Phys. **318**, 71 (2005).

[8] A. Pandey and P. Guyot-Sionnest, J. Chem. Phys. **127**, 111104 (2007).

[9] A. Creti, M. Anni, M. Z. Rossi, G. Lanzani, L. Manna, and M. Lomascolo, Appl. Phys. Lett. **91**, 093106 (2007).

[10] V. Barzykin and M. Tachiya, J. Phys. Condens. Matter **19**, 065105 (2007).

[11] A. Ueda, T. Tayagaki, and Y. Kanemitsu, J. Phys. Soc. Jpn. **78**, 083706 (2009).

[12] I. Robel, R. Gresback, U. Kortshagen, R. D. Schaller, and V. I. Klimov, Phys. Rev. Lett. **102**, 177404 (2009).

[13] Y. Kobayashi, L. Pan, and N. Tamai, J. Phys. Chem. C **113**, 11783 (2009).

[14] J. J. H. Pijpers, M. T. W. Milder, C. Delerue, and M. Bonn, J. Phys. Chem. C **114**, 6318 (2010).

[15] S. Taguchi, A. Ishizumi, and Y. Kanemitsu, J. Phys. Soc. Jpn. **79**, 063710 (2010).

[16] R. D. Schaller and V. I. Klimov, Phys. Rev. Lett. **92**, 186601 (2004).

[17] R. J. Ellingson, M. C. Beard, J. C. Johnson, P. Yu, O. I. Micic, A. J. Nozik, A. Shabaev, and Al. L. Efros, Nano Lett. **5**, 865 (2005).

[18] G. Nair, S. M. Geyer, L. Y. Chang, and M. G. Bawendi, Phys. Rev. B **78**, 125325 (2008).

[19] A. Ueda, K. Matsuda, T. Tayagaki, and Y. Kanemitsu, Appl. Phys. Lett. **92**, 233105 (2008).

[20] J. J. H. Pijpers, R. Ulbricht, K. J. Tielrooij, A. Osherov, Y. Golan, C. Delerue, G. Allan, and M. Bonn, Nature Phys. **5**, 811 (2009).

[21] D. I. Chepic, Al. L. Efros, A. I. Ekimov, M. G. Ivanov, V. A. Kharchenko, I. A. Kudriavtsev, and T. V. Yazeva, J. Lumin. **47**, 113 (1990).

[22] M. Nirmal, B. O. Dabbousi, M. G. Bawendi, J. J. Macklin, J. K. Trautman, T. D. Harris, and L. E. Brus, Nature (London) **383**, 802 (1996).

[23] M. Kuno, D. P. Fromm, H. F. Hamann, A. Gallagher, and D. J. Nesbitt, J. Chem. Phys. **115**, 1028 (2001).

[24] Al. L. Efros and M. Rosen, Phys. Rev. Lett. **78**, 1110 (1997).

[25] Y. Kanemitsu, S. Okamoto, M. Otobe, and S. Oda, Phys. Rev. B **55**, R7375 (1997).

[26] M. A. Hines and P. Guyot-Sionnest, J. Phys. Chem. **100**, 468 (1996).

[27] B. O. Dabbousi, J. Rodriguez-Viejo, F. V. Mikulec, J. R. Heine, H. Mattoussi, R. Ober, K. F. Jensen, and M. G. Bawendi, J. Phys. Chem. B **101**, 9463 (1997).

[28] K. T. Shimizu, W. K. Woo, B. R. Fisher, H. J. Eisler, and M. G. Bawendi, Phys. Rev. Lett. **89**, 117401 (2002).

[29] Y. Ito, K. Matsuda, and Y. Kanemitsu, Phys. Rev. B **75**, 033309 (2007).

[30] F. Cichos, C. von Borczyskowski, and M. Orrit, Curr. Opin. Colloid Interface Sci. **12**, 272 (2007).

[31] X. Wang, X. Ren, K. Kahen, M. A. Hahn, M. Rajeswaran, S. Maccagnano-Zacher, J. Silcox, G. E. Cragg, Al. L. Efros, and T. D. Krauss, Nature (London) **459**, 686 (2009).

[32] R. Osovsky, D. Cheskis, V. Kloper, A. Sashchiuk, M. Kroner, and E. Lifshitz, Phys. Rev. Lett. **102**, 197401 (2009).

[33] G. E. Cragg and Al. L. Efros, Nano Lett. **10**, 313 (2010).

[34] H. Htoon, J. A. Hollingsworth, R. Dickerson, and V. I. Klimov, Phys. Rev. Lett. **91**, 227401 (2003).

[35] I. Robel, B. A. Bunker, P. V. Kamat, and M. Kuno, Nano Lett. **6**, 1344 (2006).

[36] Z. A. Peng and X. Peng, J. Am. Chem. Soc. **124**, 3343 (2002).

[37] Y. A. Yang, H. Wu, K. R. Williams, and Y. C. Cao, Angew. Chem. Int. Ed. **44**, 6712 (2005).

[38] J. I. Kim and J. Lee, Adv. Funct. Mater. **16**, 2077 (2006).

[39] X. Zhong, Y. Feng, and Y. Zhang, J. Phys. Chem. C **111**, 526 (2007).

[40] L. Liu, Z. Zhuang, T. Xie, Y. G. Wang, J. Li, Q. Peng, and Y. Li, J. Am. Chem. Soc. **131**, 16423 (2009).

[41] J. Hu, L. Li, W. Yang, L. Manna, L. Wang, and A. P. Alivisatos, Science **292**, 2060 (2001).

[42] G. Schlegel, J. Bohnenberger, I. Potapova, and A. Mews, Phys. Rev. Lett. **88**, 137401 (2002).

[43] As an example, *Phosphor Handbook*, 2nd ed. edited by W. M. Yen, S. Shionoya, and H. Yamamoto (CRC Press, Boca Raton, FL, 2006).

[44] V. I. Klimov, C. J. Schwarz, D. W. McBranch, C. A. Leatherdale, and M. G. Bawendi, Phys. Rev. B **60**, R2177 (1999).

[45] R. G. Ispasoiu, J. Lee, F. Papadimitrakopoulos, and T. Goodson III, Chem. Phys. Lett. **340**, 7 (2001).

[46] Z. Jiang and D. F. Kelley, J. Phys. Chem. C **114**, 17519 (2010).

[47] M. Jones, S. S. Lo, and G. D. Scholes, Proc. Natl. Acad. Sci. USA **106**, 3011 (2009).

[48] M. Achermann, J. A. Hollingsworth, and V. I. Klimov, Phys. Rev. B **68**, 245302 (2003).

[49] M. R. Junnarkar and R. R. Alfano, Phys. Rev. B **34**, 7045 (1986)

[50] P. T. Landsberg, *Recombination in Semiconductors* (Cambridge University Press, Cambridge, 1991).